

Metallicity Evolution of Damped Lyman-Alpha Galaxies

Varsha P. Kulkarni

Dept. of Physics & Astronomy, University of South Carolina, Columbia, SC 29208

S. Michael Fall

Space Telescope Science Institute, 3700 San Martin Drive, Baltimore, MD 21218

ABSTRACT

We have reanalyzed the existing data on Zinc abundances in damped Ly α (DLA) absorbers to investigate whether their mean metallicity evolves with time. Most models of cosmic chemical evolution predict that the mass-weighted mean interstellar metallicity of galaxies should rise with time from a low value $\sim 1/30$ solar at $z \sim 3$ to a nearly solar value at $z \sim 0$. However, several previous analyses have suggested that there is little or no evolution in the global metallicity of DLAs. The main problem is that the effective number of systems that dominate the $N(\text{HI})$ -weighted mean metallicity is very small.

We have used a variety of statistical techniques to quantify the global metallicity-redshift relation and its uncertainties, taking into account both measurement and sampling errors. Three new features of our analysis are: (a) an unbinned $N(\text{HI})$ -weighted nonlinear χ^2 fit to an exponential relation; (b) survival analysis to treat the large number of limits in the existing data; and (c) a comparison of the data with several models of cosmic chemical evolution based on an unbinned $N(\text{HI})$ -weighted χ^2 . We find that a wider range of evolutionary rates is allowed by the present data than claimed in previous studies. The slope of the exponential fit to the $N(\text{HI})$ -weighted mean Zn metallicity vs. redshift relation is -0.20 ± 0.11 counting limits as detections and -0.27 ± 0.12 counting limits as zeros. Similar results are also obtained if the data are binned in redshift, and if survival analysis is used. These slopes are marginally consistent with no evolution, but are also consistent with the rates predicted by several models of cosmic chemical evolution (e.g., slopes of -0.61 to -0.25 for the models of Pei & Fall 1995, Malaney & Chaboyer 1996, and Pei et al. 1999). The χ^2 values obtained for most of these models are somewhat worse than that for the exponential model because the models lie above the observed data points, but still suggest

that the present DLA data could indicate some evolution of the metallicity with redshift. Finally, we outline some future measurements necessary to improve the statistics of the global metallicity-redshift relation.

Subject headings: quasars: absorption lines; galaxies: evolution; galaxies: abundances; cosmology: observations

1. INTRODUCTION

The evolution of stars and gas in galaxies are topics of great interest in modern astrophysics. The average star-formation history of the universe has been estimated from emission properties of galaxies detected in deep imaging and redshift surveys (e.g. Lilly et al. 1996; Madau et al. 1996, 1998). This emission history of galaxies is connected intimately with the histories of gas consumption and metal production, because the global densities of gas, metals, and stars are coupled through conservation-type relations (e.g., Fall 2001). In particular, because the global rate of star formation is known to be high at $1 \lesssim z \lesssim 4$, we expect the mean interstellar metallicity of galaxies to rise rapidly in that interval. Direct observational constraints on the evolution of the mean metallicity in galaxies are therefore important for pinning down the histories of star formation and gas consumption.

Abundance measurements in gas traced by quasar absorption lines can directly probe the evolution of metals in galaxies. The damped Ly α (DLA) absorbers ($\log N(\text{HI}) \gtrsim 20$) are particularly important, since they contain a large fraction of the neutral gas in galaxies, nearly enough to form all of the stars visible today (e.g., Wolfe et al. 1995). DLAs are the only class of high-redshift objects in which abundances of a large number of elements have been measured (e.g., Meyer & York 1992; Pettini et al. 1994, 1997, 1999, 2000; Lu et al. 1996; Kulkarni et al. 1996, 1997, 1999; Prochaska & Wolfe 1996, 1997, 1999; Prochaska et al. 2001b; and references therein). In previous studies, Zn II has been the most commonly used ion for estimating the total (gas + solid phase) metallicity in DLAs, for a number of reasons: (1) Zn is relatively undepleted on interstellar dust grains; (2) it tracks Fe closely in Galactic stars (for $[\text{Fe}/\text{H}] \gtrsim -2$); (3) its absorption lines are usually unsaturated and often lie outside the Ly α forest; and (4) ionization corrections are relatively small for Zn II. Abundances of depleted elements such as Cr or Fe relative to Zn are used to estimate the dust content of DLAs.

The quantity of interest here is the $N(\text{HI})$ -weighted mean metallicity, which corresponds to the global $\Omega_{\text{metals}}^{\text{ISM}}/\Omega_{\text{gas}}^{\text{ISM}}$ ratio in galaxies. The average interstellar properties of galaxies can be determined from the statistics of quasar absorption-line systems as follows. Let $f(N_x, z)$

be the distribution in column density and redshift, for particles of any type x that absorb or scatter light. These might, for example, be hydrogen atoms ($x = \text{H I}$), metal ions ($x = m$), or dust grains ($x = d$). By definition, $H_0(1+z)^3|dt/dz|f(N_x, z)dN_x dz$ is the mean number of absorption-line systems with column densities of x between N_x and $N_x + dN_x$ and redshifts between z and $z + dz$ along the lines of sight to randomly selected background quasars. These lines of sight are very narrow (the projected size of the continuum-emitting regions of quasars, less than a light-year across) and pierce the absorption-line systems at random angles and impact parameters. One can show that the mean comoving density of x is given by

$$\Omega_x(z) = \frac{8\pi G m_x}{3cH_0} \int_0^\infty N_x f(N_x, z) dN_x, \quad (1)$$

where m_x is the mass of a single particle (atom, ion, or grain). Equation (1) plays a central role in this subject. It enables us to estimate the mean comoving densities of many quantities of interest without knowing anything about the structure of the absorption-line systems. In particular, we do not need to know their sizes or shapes, whether they are smooth or clumpy, and so forth. Furthermore, in the absence of selection biases, equation (1) gives exactly the correct weighting to lines of sight at different impact parameters, i.e. distances from the centers of galaxies. This point is sometimes confused in the literature and even the opposite is sometimes asserted (e.g., Edmunds & Phillips 1997). A corollary of equation (1) is that the global interstellar metallicity, $Z \equiv \Omega_{\text{metals}}^{\text{ISM}}/\Omega_{\text{gas}}^{\text{ISM}}$, is given simply by an average over the metallicities of individual absorption-line systems weighted by their H I column densities.

Most models of cosmic chemical evolution predict that the global interstellar metallicity rises with time, from a low value at high redshifts to a near-solar value at zero redshift (e.g., Lanzetta, Wolfe, & Turnshek 1995; Pei & Fall 1995; Malaney & Chaboyer 1996; Pei, Fall, & Hauser 1999; Tissera et al. 2001). Moreover, from emission-line observations of nearby galaxies, it appears that the present-day mass-weighted mean interstellar metallicity of galaxies, averaged over all morphological types, is near-solar. We show this explicitly in the Appendix using the mean relation between galaxy luminosity and interstellar metallicity as derived from H II regions, and integrating over the luminosity function of galaxies. However, it is not clear from the absorption-line observations whether or not the mean metallicity in DLAs actually increases with decreasing redshift as predicted by the models.

There have been several attempts to estimate the $N(\text{H I})$ -weighted mean Zn metallicity of DLAs at $0.4 \lesssim z \lesssim 3.5$ (e.g., Pettini et al. 1997, 1999; Vladilo et al. 2000; Savaglio 2001). These studies have claimed that there is little or no evolution in the global Zn metallicity of DLAs in this redshift range. Prochaska & Wolfe (1999, 2000, 2002) and Prochaska, Gawiser, & Wolfe (2001a) have found no evolution in the mean Fe abundance for $2 \lesssim z \lesssim 4$. However, these previous studies have not made consistent quantitative estimates of the mean slope of

the global metallicity-redshift relation and the observational uncertainties in that relation. There are, in fact, several uncertainties in the present DLA metallicity data. First of all, the metallicities for individual DLAs show a large intrinsic or cosmic scatter at any given redshift, reflecting the different rates of chemical enrichment of different galaxies. Furthermore, the current samples are relatively small. More importantly, the estimates of the $N(\text{HI})$ -weighted mean metallicity for these samples are dominated by only the few DLAs with the highest $N(\text{HI})$. To discriminate between evolution vs. no evolution from these intrinsically noisy samples, it is crucial to estimate quantitatively the mean metallicity-redshift relation and the effect of the observational uncertainties on that relation. Here we present a reexamination of the Zn data with quantitative estimates of the mean metallicity-redshift relation and comparison with predictions of cosmic chemical evolution models. We include several recent low-redshift measurements, which are crucial for determining the slope of the metallicity-redshift relation. Using a number of different statistical techniques, we find that the existing data could support significant evolution of the global metallicity with redshift.

2. ANALYSIS AND RESULTS

To set the stage for our analysis, we begin by giving an overview of the previous studies of the global metallicity-redshift relation for the DLAs. Table 1 compares the different studies in terms of the elements used, the number of detections and upper limits included, the way the limits were treated, the redshift range covered, whether the data were binned, whether the errors in the $N(\text{HI})$ -weighted means were calculated consistently, whether the slope was quantified, and finally, the conclusions that were reached regarding metallicity evolution. Here we have not included studies of unweighted mean metallicities, since these are not appropriate for estimates of the global metallicity-redshift relation. Savaglio (2001) has reported that the subsample of low- $N(\text{HI})$ DLAs shows some metallicity evolution. We do not include this result in Table 1 since such a subsample does not give the total global metallicity.

It is clear from Table 1 that most previous studies did not determine the slope of the global metallicity vs. redshift relation. The only one that did estimate the slope underestimated the uncertainties (by giving equal weight to each DLA while calculating the errors in the $N(\text{HI})$ -weighted mean metallicities). Our study (summarized in the last line of Table 1) presents a more rigorous and quantitative analysis of the data and shows that contrary to the no-evolution picture suggested by most researchers in this field, the current data are actually consistent with substantial evolution of the metallicity with redshift.

For this study, we use only Zn measurements, because this provides us with a large

sample spanning a relatively wide redshift range and allows us to analyze the data uniformly without having to correct for dust depletion. (See section 3 for a more detailed discussion of this point.) Using Zn alone and excluding Fe does limit the size of our samples at $z > 3$, but that redshift range corresponds to only 16% of the age of the universe¹. We do not include DLAs with $z_{\text{abs}} \approx z_{\text{em}}$ in broad absorption line (BAL) quasars, since these are thought to contain matter outflowing from the quasars, rather than typical galactic interstellar matter. We also eliminate DLAs with uncertain or unavailable H I column densities. Our samples include Zn measurements from Meyer & York (1992); Meyer et al. (1995); Lu et al. (1995, 1996); Boisse et al. (1998); Pettini et al. (1994, 1997, 1999, 2000); Prochaska & Wolfe (1996, 1997, 1999); Lopez et al. (1999, 2002); de la Varga et al. (2000); Petitjean, Srianand, & Ledoux (2000); Molaro et al. (2001); Ellison & Lopez (2001); Prochaska et al. (2001b); and Levshakov et al. (2002). In addition, we also include results from a survey of DLA abundances for $0.6 < z < 2.3$, performed with the Multiple Mirror Telescope (Kulkarni, Bechtold, & Ge 1999; Ge, Bechtold, & Kulkarni 2001). This is the complete list of published measurements, to our knowledge, as of 2002 June 20. Together these represent 36 detections and 21 limits. More than 80% of the limits are 3σ , while the rest are 4σ . The interested reader can access our samples at <http://boson.physics.sc.edu/~kulkarni/DLAZndata.html>.

We now describe our analysis for the trends in the global metallicity based on these samples. We assume throughout that Zn is not depleted and is a good indicator of metallicity. Furthermore, we assume that most of the hydrogen in the DLAs is neutral and atomic (H I) while most of the Zn is singly ionized (Zn II). These are standard assumptions also made in previous studies in this field. The metallicity of an individual DLA is thus approximated by

$$Z_i = \frac{N(\text{Zn II})_i / N(\text{H I})_i}{(\text{Zn/H})_{\odot}} Z_{\odot}, \quad (2)$$

where $Z_{\odot} = 0.02$ is the present-day solar metallicity, and $(\text{Zn/H})_{\odot} = 10^{-7.35}$ is the solar Zn fraction (Anders & Grevesse 1989). The $N(\text{H I})$ -weighted mean metallicity \bar{Z} in a sample of DLAs is then given by

$$\bar{Z} = \frac{\sum N(\text{Zn II})_i / \sum N(\text{H I})_i}{(\text{Zn/H})_{\odot}} Z_{\odot}. \quad (3)$$

This can be reexpressed in the more familiar form of a weighted mean

$$\bar{Z} = \sum w_i Z_i, \quad (4)$$

where the normalized weighting factors

$$w_i = N(\text{H I})_i / \sum N(\text{H I})_i \quad (5)$$

¹Throughout this article, we compute fractions of the age of the universe using the “concordance” cosmological parameters $\Omega_m = 0.3$ and $\Omega_{\Lambda} = 0.7$.

are the fractional contributions of the individual DLAs to the total H I column density of the sample. We quantify the evolution of \bar{Z} , first without binning the data, and then with a binned approach for the purpose of pictorial presentation.

2.1. The Unbinned Approach

Here, we fit a simple model $\bar{Z}_p(z)$ to the individual metallicities Z_i by the method of weighted nonlinear least squares. This is the first study to use such an unbinned approach for the analysis of DLA metallicity evolution. Thus, we minimize the quantity

$$\chi^2 = \sum w_i \left[\frac{Z_i - \bar{Z}_p(z_i)}{\sigma_Z} \right]^2, \quad (6)$$

where the weights w_i are given by equation (5). It can be verified that minimization of the χ^2 thus defined gives the same results as a binned approach in the hypothetical limiting case of a flat mean metallicity-redshift relation, $\bar{Z}_p(z) = \text{const}$.

For the sake of definiteness, we assume that the models $\bar{Z}_p(z)$ can be specified with two parameters, and denote by $\bar{Z}_p^{\text{best}}(z)$ the best-fit model corresponding to those values of the parameters that minimize the χ^2 . The quantity σ_Z in equation (6) is a measure of the scatter among the observed metallicities Z_i with respect to the mean trend.² We take σ_Z as the scatter with respect to the best-fit model:

$$\sigma_Z^2 = \frac{\sum w_i [Z_i - \bar{Z}_p^{\text{best}}(z_i)]^2}{(n - 2)}. \quad (7)$$

Thus, by definition, the best-fit model has a reduced chi-square (χ_ν^2) of 1. It is, therefore, not possible to get an independent estimate of the goodness of fit. But the contour corresponding to $\chi^2 = \chi_{\text{min}}^2 + 1$ can be used to obtain error bars on the parameters of the model $\bar{Z}_p(z)$.

2.1.1. Exponential Models

The few previous studies that have attempted to quantify the observed shape of the metallicity-redshift relation have fitted a straight line to the logarithm of the mean metallicity vs. redshift data, of the form

$$\log \bar{Z} = \log \bar{Z}_0 + bz. \quad (8)$$

²Note that we cannot use the measurement errors to calculate σ_Z , because they are small compared to the scatter in the data.

The corresponding expression for the mean metallicity itself has an exponential dependence on redshift:

$$\bar{Z}_p(z) = \bar{Z}_0 \exp(-az), \quad (9)$$

where $a = -b \ln(10)$. In fact, as we will discuss below and illustrate in Fig. 1, most models of cosmic chemical evolution also predict a roughly exponential increase in the mean metallicity with decreasing redshift over the range of the DLA Zn observations. Therefore, we begin our analysis by assuming an exponential form for the predicted metallicity for easy comparison with previous studies. We then follow this in section 2.3 with more detailed comparisons with the predictions of several models of cosmic chemical evolution. The best-fitting values of the parameters \bar{Z}_0 and a can be obtained by minimizing χ^2 numerically, using equations (6) and (9). The 1σ errors in \bar{Z}_0 and a can then be estimated using equations (6), (7), and (9), from the contour in the $\bar{Z}_0 - a$ plane corresponding to $\chi^2 = \chi_{\min}^2 + 1$.

The situation is complicated somewhat by the large number of upper limits on the Zn II column densities in the current samples. Although a rigorous way to perform linear unweighted regression with both detections and limits is using survival analysis, to our knowledge, no statistical techniques have been developed as yet for nonlinear weighted regression using survival analysis. Therefore, we consider two extreme cases to take account of the upper limits. We first treat the upper limits as detections, and obtain the intercept $\log(\bar{Z}_0/Z_\odot) = -0.71 \pm 0.20$ and the slope $b = -0.20 \pm 0.11$ for the logarithmic mean metallicity vs. linear redshift relation. In the opposite extreme, we treat the upper limits as zeros and obtain $\log(\bar{Z}_0/Z_\odot) = -0.64 \pm 0.20$ and $b = -0.27 \pm 0.12$. (The errors in the slope and intercept are, of course, closely correlated.) These results are summarized in Table 3. The slopes differ from zero at $\approx 2\sigma$ levels, suggesting that the present data could support evolution of the mean metallicity with redshift. The intercepts $\log(\bar{Z}_0/Z_\odot)$ differ from zero at $> 3\sigma$ levels. But this is not a serious problem because the intercepts involve an extrapolation outside the redshift range of the available data.

2.2. The Binned Approach

We now consider the binned approach for the purpose of pictorial presentation. We divide the sample into five redshift bins with roughly equal numbers of DLAs per bin. For each redshift bin, the error in the $N(\text{HI})$ -weighted mean metallicity \bar{Z} can be calculated by using the standard expressions for the weighted mean and its sampling and measurement errors (e.g., Bevington & Robinson 1992). The Poisson statistical error in the weighted

mean, because of the finite size of the sample, is given by

$$\sigma^2(\bar{Z})_{\text{samp}} = \frac{\Sigma[w_i(Z_i - \bar{Z})^2]}{(n - 1)}, \quad (10)$$

where n is the number of measurements in a given bin.

It is informative to note that equation (10) can also be rewritten as

$$\sigma^2(\bar{Z})_{\text{samp}} = \frac{\Sigma(Z_i - \bar{Z}')^2}{n_{\text{eff}}(n_{\text{eff}} - 1)}, \quad (11)$$

where $\bar{Z}' = \Sigma Z_i/n$ is the unweighted mean metallicity, and n_{eff} , the effective number of DLAs, is given by

$$n_{\text{eff}} = \frac{1}{2} \left\{ 1 + \left[1 + \frac{4(n - 1)[\Sigma(Z_i - \bar{Z}')^2]}{\Sigma w_i(Z_i - \bar{Z}')^2} \right]^{1/2} \right\}. \quad (12)$$

If all the weights w_i were equal, n_{eff} would be equal to n , \bar{Z}' would be equal to \bar{Z} , and $\sigma(\bar{Z})_{\text{samp}}$ would be the usual standard deviation among the values Z_i , divided by \sqrt{n} . However, with unequal weights, the effective number of systems n_{eff} is smaller than n , and the weighted mean is dominated by only the few DLAs with the largest $N(\text{HI})$.

The other source of uncertainty in \bar{Z} is the measurement error in the individual values of $N(\text{HI})$ and $N(\text{Zn II})$. The median measurement errors in the H I column densities are 20%, but there is a wide range with $\approx 80\%$ of the values in the range 12 – 26%. The median measurement errors in the Zn II column densities are 25%, with $\approx 80\%$ of the values in the range 7 – 40%. (In general, the errors from observations obtained at eight-meter class telescopes are smaller than those from observations at four-meter class telescopes.) For any given DLA, the measurement errors in $N(\text{HI})$ and $N(\text{Zn II})$ are expected to be uncorrelated, since these quantities are derived from independent measurements of the H I Ly- α line and the Zn II lines. We therefore evaluate the effect of these individual measurement errors on the $N(\text{HI})$ -weighted mean metallicity \bar{Z} , using the standard formula for error propagation:

$$\sigma^2(\bar{Z})_{\text{meas}} = \Sigma \left[\frac{\partial \bar{Z}}{\partial N(\text{Zn II})_i} \right]^2 \sigma^2[N(\text{Zn II})_i] + \Sigma \left[\frac{\partial \bar{Z}}{\partial N(\text{HI})_i} \right]^2 \sigma^2[N(\text{HI})_i]. \quad (13)$$

Using equations (3) and (13), we get

$$\sigma^2(\bar{Z})_{\text{meas}} = \frac{[Z_{\odot}/(\text{Zn}/\text{H})_{\odot}]^2 \Sigma \sigma^2[N(\text{Zn II})_i] + \bar{Z}^2 \Sigma \sigma^2[N(\text{HI})_i]}{[\Sigma N(\text{HI})_i]^2}. \quad (14)$$

The combined uncertainty in \bar{Z} is given by

$$\sigma^2(\bar{Z})_{\text{tot}} = \sigma^2(\bar{Z})_{\text{samp}} + \sigma^2(\bar{Z})_{\text{meas}}. \quad (15)$$

Finally, the uncertainty in the logarithmic $N(\text{HI})$ -weighted mean metallicity is given approximately by

$$\sigma[\log(\bar{Z}/Z_{\odot})]_{\text{tot}} = \frac{1}{2} \left\{ \log[\bar{Z} + \sigma(\bar{Z})_{\text{tot}}] - \log[\bar{Z} - \sigma(\bar{Z})_{\text{tot}}] \right\}. \quad (16)$$

2.2.1. The Maximum and Minimum Limits Cases

To estimate the $N(\text{HI})$ -weighted mean metallicity and its uncertainty in each redshift bin, we again consider two extreme cases allowed by the existing observations where the limits are treated either as detections (the “maximum limits” case) or as zeros (the “minimum limits” case). These two cases provide strict upper and lower limits to the mean metallicity in each redshift bin, as verified by the survival analysis in section 2.2.2 below. Table 2 lists the results for each bin obtained in these two cases. Figure 1 shows the logarithmic $N(\text{HI})$ -weighted mean metallicity relative to the solar value and its 1σ uncertainties, obtained as described above for our samples, as a function of redshift. Each point is plotted at the median redshift for the respective bin. Horizontal bars indicate the full range of redshifts of the DLAs in each bin. The left and right panels refer, respectively, to the cases of maximum and minimum limits. It is interesting to note that the mean metallicities and the relative trend with redshift do not change much whether the limits are treated as detections or zeros. This is because the mean metallicity in each bin is dominated by the high- $N(\text{HI})$ systems, for which the Zn values are invariably detections rather than limits. (This also clarifies that the intrinsic weakness of the Zn lines—compared to say Fe lines—is not a serious problem in the estimation of the global metallicity.) The vertical error bars show the total uncertainties $\sigma[\log(\bar{Z}/Z_{\odot})]_{\text{tot}}$, including both the sampling errors, reflecting the scatter among individual DLAs, and the measurement errors in the column densities. The sampling errors are found to be the dominant source of uncertainty, making up $\gtrsim 85\%$ of the total error in each bin. The horizontal dashed line at $\bar{Z} = Z_{\odot}$ denotes the solar value. The curves in Figure 1 are the predictions of cosmic chemical evolution models and will be discussed in section 2.3.

As for the unbinned approach, for easy comparison with the few previous studies that quantified the chemical evolution of DLAs, we fit a linear relation of the form of equation (8) to the observed logarithmic mean metallicity vs. redshift data. Based on linear regression, we obtain $\log(\bar{Z}_0/Z_{\odot}) = -0.76 \pm 0.27$ and $b = -0.16 \pm 0.12$, counting the limits as detections, and $\log(\bar{Z}_0/Z_{\odot}) = -0.72 \pm 0.30$ and $b = -0.23 \pm 0.15$, counting the limits as zeros.³

³Unlike the case of the means in the individual redshift bins, the true ranges of the slope and the intercept are not necessarily bracketed by the minimum and maximum limits, but these two cases are indicative of the ranges the slope and the intercept are likely to take.

These results are also summarized in Table 3. ⁴ χ^2_ν for the optimum fits to the binned data is 0.47 counting the limits as detections, and 0.51 counting the limits as zeros, with the corresponding probabilities $P(\chi^2_\nu \geq \chi^2_{\nu, \min})$ of 0.93 and 0.92, respectively.

2.2.2. Survival Analysis

Although the difference between the maximum limits and minimum limits cases is small, a more rigorous treatment of the limits can be achieved by using techniques of survival analysis for censored data (i.e. data with limits). We therefore also analyze the DLA Zn data using survival analysis. We use the Kaplan-Meier (K-M) non-parametric estimator, which is often used in biostatistics and has also been used in some astronomical applications with upper limits. We compute the mean metallicity in each redshift bin with the K-M estimator, using the astronomical survival analysis package ASURV rev. 1.2 (Isobe & Feigelson 1990) which implements the methods presented in Feigelson & Nelson (1985) for univariate problems. The last column in Table 2 lists the logarithmic $N(\text{HI})$ -weighted mean metallicity for the five redshift bins, as obtained from survival analysis. As expected, these values lie in between the corresponding values for the maximum and minimum limits cases. ⁵ Linear regression of these binned data yields an intercept $\log(\bar{Z}_0/Z_\odot) = -0.64 \pm 0.20$ and a slope $b = -0.26 \pm 0.10$ for the metallicity vs. redshift relation (see Table 3). The results of the survival analysis thus confirm the estimates from the cases of maximum and minimum limits.

⁴Recently, measurements of X-ray absorption lines have been used to estimate the metallicities of two DLAs at $z = 0.313$ and $z = 0.524$ (Bechtold et al. 2001; Junkkarinen et al. 2002). We have not included these in our sample, because there are no published Zn metallicities for these objects yet, and there could be a systematic difference between the Zn and X-ray-based metallicities. However, if we count these two systems in the lowest redshift bin, using the X-ray-based metallicities, the binned estimates of the intercept and the slope of the metallicity-redshift relation are $\log(\bar{Z}_0/Z_\odot) = -0.30 \pm 0.21$ and $b = -0.36 \pm 0.10$ for the maximum limits sample.

⁵The error bars on the mean metallicity in each bin for the survival analysis reflect only the sampling errors. We do not estimate the measurement errors in this case, because, to our knowledge, no method has been developed as yet for rigorously incorporating measurement errors into survival analysis with limits and detections. However, this is not a significant problem considering that $\gtrsim 85\%$ of the contribution to the errors arises in the sampling errors for the maximum and minimum limits cases.

2.3. Comparison of Data with Models

The exponential form assumed above for the mean metallicity vs. redshift relation is of course an approximation, although convenient for purposes of comparison with previous studies. The true metallicity-redshift relation could be more complicated than this simple exponential form. Prochaska & Wolfe (2000, 2002) and Prochaska et al. (2001a) have found a flat logarithmic mean metallicity vs. redshift relation for Fe for $2 \lesssim z \lesssim 4$. It may indeed be that the metallicity rises relatively slowly at high redshifts, but more steeply at low redshifts. With this in mind, we now compare the data with several models of cosmic chemical evolution. Very few of the previous studies have made even a graphical comparison between the models and the data. (The exceptions are Pei et al. 1999 and Savaglio 2001.)

The dotted, short-dashed, solid, and long-dashed curves in Figure 1 show, respectively, (a) the mean interstellar metallicity in the closed-box and outflow models of Pei & Fall (1995); (b) the mean Zn metallicity in the Malaney & Chaboyer (1996) model with a constant Zn yield, a slope of -1.70 for the initial mass function (IMF), and the evolution of the neutral gas density as computed by Pei & Fall (1995); (c) the mean interstellar metallicity in the Pei et al. (1999) model with the optimum fit for the cosmic infrared background intensity; and (d) the mean metallicity of cold interstellar gas in the collisional star-burst model of Somerville, Primack, & Faber (2001). The metallicity evolution of the models clearly depends on several input parameters, such as the IMF slope, the Zn yields, and the star formation history of the galaxies. All of these models have near-solar metallicity at the present epoch, as required by the observed present-day mean interstellar metallicity of galaxies (see the Appendix). However, the models with shallower slopes tend to lie above the DLA data at $z \sim 2$, while the models with steeper slopes tend to go through the DLA data at $z \sim 2$.

In the redshift range where the data and the models can be compared, the average slopes for the Pei & Fall (1995) models are -0.54 to -0.42 , while the slopes for the Malaney & Chaboyer (1996) models are -0.45 to -0.25 . The models of Pei et al. (1999) predict slopes of -0.61 to -0.45 . The hydrodynamical simulations of star formation and metal production in hierarchical clustering scenarios by Tissera et al. (2001) predict a slope of -0.33 for the mass-weighted mean logarithmic metallicity as a function of redshift. The semi-analytic collisional star-burst model for galaxy formation in the cold dark matter cosmogony by Somerville et al. (2001) predicts a slope of -0.21 for the mean metallicity of cold interstellar gas as a function of redshift (but predicts higher metallicities at all redshifts than observed for DLAs). The slopes of the observed mean metallicity-redshift relation (from Table 3) are marginally consistent with no evolution, but also agree, within $\approx 2\sigma$, with most of the model predictions.

To quantify the comparison of the data with the models of cosmic chemical evolution,

we now compare the weighted χ^2 for the unbinned data, following equation (6), with \bar{Z}_p in this case given by the cosmic chemical evolution models. The weights w_i are, once again, the fractional contributions of the individual DLAs to the total $N(\text{HI})$ of the entire sample. As before, we calculate σ_Z as the scatter in the data with respect to the best exponential fit (as determined in section 2.1). The χ^2 thus defined cannot give us independent estimates of the goodness of fit of each model. But the relative values of χ^2 can be used to compare how well the models fit the data.

Table 4 lists χ_ν^2 for each of the four models shown in Figure 1 with respect to the unbinned data. Also listed are the corresponding values for the Pei et al. (1999) models for the maximum and minimum allowed fits to the cosmic infrared background intensity. On the same scale, the corresponding value of χ_ν^2 for the best exponential fit is 1 by definition. Even though the χ_ν^2 values in Table 4 do not reflect the goodness of fit in an absolute sense, they are roughly similar to the values expected on the basis of the comparison of the curves in Figure 1 with the binned data points. The main reason for the higher values of χ_ν^2 for the chemical evolution models than for the exponential fit is that the models lie above the data points. The Malaney & Chaboyer (1996) and Somerville et al. (2001) models have shallower slopes than the other models, but their offset to higher metallicities give them worse χ_ν^2 , as evident from Figure 1. Overall, we conclude that at least some of the chemical evolution models are consistent with the DLA data, supporting some evolution in the global metallicity as a function of redshift. We note, however, that dust in DLA galaxies can introduce a systematic selection bias in the observed mean metallicity. The curves plotted in Figure 1 have not been corrected for this bias. We discuss this point further in section 3.1. In future, when more measurements at low redshifts become available, it should be possible to make more stringent comparisons of the models with the data.

3. DISCUSSION

Most previous studies have claimed that there is no evolution in the global metallicity of DLAs. However, these studies have not been definitive for various reasons summarized in Table 1. Our analysis has demonstrated that the present DLA Zn data are consistent with some evolution of the global interstellar metallicity. The main reason for the large uncertainties is that the effective number of measurements that dominate the $N(\text{HI})$ -weighted mean metallicity is very small.

A complete lack of evolution in the mean metallicity would be quite surprising. Such a trend would be hard to reconcile with the inference that the global rate of star formation was high at $1 \lesssim z \lesssim 4$, based on the luminosity density of galaxies observed in deep surveys such

as the Canada-France Redshift Survey and the Hubble Deep Field (e.g. Lilly et al. 1996; Madau et al. 1996, 1998). The metallicity of interstellar matter in galaxies is thus expected to rise with time. Indeed, the census of the metals in nearby galaxies shows a luminosity-weighted mean interstellar metallicity close to the solar value. (See the Appendix.) DLAs are believed to represent the interstellar matter of galaxies, and are therefore expected to show an increase in the mean metallicity with decreasing redshift. As we have shown, the DLA data are, in fact, consistent with the metallicity evolution predicted by some cosmic chemical evolution models.

3.1. Dust Obscuration Bias

Dust in DLA galaxies could bias the empirical estimates of the mean metallicity \bar{Z} and its evolution with redshift. This is because the DLA galaxies with the highest column densities of metals are likely to be those with the highest column densities of dust, and these may obscure background quasars to such a degree that some of them are omitted from optically selected samples (Fall & Pei 1993; Boisse et al. 1998). Evidence for dust in DLA galaxies comes from the statistical reddening of background quasars (Fall, Pei, & McMahon 1989; Pei, Fall, & Bechtold 1991) and the depletion patterns of heavy elements, especially Zn and Cr (e.g., Pettini et al. 1994, 1997). Like the mean metallicity, the mean dust-to-gas ratio in the observed DLA galaxies is low at high redshifts, where most of the measurements have been made. The mean dust-to-metals ratio appears to be roughly independent of redshift and about equal to that in the Milky Way and the Magellanic Clouds (see Figure 1 of Pei et al. 1999). As a result of obscuration, the observed mean metallicity in the DLA galaxies, and hence the data points in Figure 1, may lie systematically below the true mean metallicity. The curves in Figure 1, however, are predictions for the true mean metallicity, without corrections for obscuration, from the models of cosmic chemical evolution.

The severity of this bias depends on several factors, including the extinction curve of the dust, the distribution of dust column densities in the DLA galaxies, the luminosity function of quasars, and the passband in which they are observed (see the Appendix of Fall & Pei 1993 for a detailed analysis). Together, these factors determine the fraction of the sky covered by dust as a function of the optical depth. The main difficulty in correcting for the bias stems from the unknown distribution of dust column densities in the DLA galaxies or, for a given (observed) distribution of H I column densities, the unknown distribution of dust-to-gas ratios. For an assumed shape of this distribution, one can, however, compute the expected bias as a function of the width of the distribution. Fall & Pei (1993) have made such calculations for a log-normal distribution of the dust-to-gas ratio k in the DLA galaxies.

They find that the true mean dust-to-gas ratio \bar{k}_t exceeds the observed mean \bar{k}_o by a factor that increases from $\bar{k}_t/\bar{k}_o = 1.2$ to 1.7 to 4 as the dispersion in the natural logarithm of the dust-to-gas ratio increases from $\sigma(\ln k) = 0.5$ to 1.0 to 1.5. This may provide an indication of the corresponding bias in the mean metallicity, since we expect $\bar{Z}_t/\bar{Z}_o \approx \bar{k}_t/\bar{k}_o$. For reference, nearby normal galaxies have $\sigma(\ln k) \approx 0.5$ (Pei 1992). Thus, if this dispersion also applies to the DLA galaxies, we might expect $\bar{Z}_t \approx \bar{Z}_o$. If the dispersion in the dust-to-gas ratio were larger, however, \bar{Z}_t could differ significantly from \bar{Z}_o .

Unfortunately, the bias caused by obscuration is difficult to quantify from theory or numerical simulation alone, because it depends on the the small-scale structure of the interstellar medium in the DLAs. Absorption-line observations sample the DLAs on scales comparable to the continuum-emitting regions of the background quasars, typically smaller, and possibly much smaller, than a light-year. Some of these lines of sight will pass through dense interstellar clouds, with high optical depths, while others, even nearby, will pass through diffuse intercloud material, with low optical depths. The obscuration of background quasars in this case may differ substantially from that in simulations with the same average interstellar density and hence optical depth but with lower spatial resolution and hence little or no structure on the relevant scales.

In principle, a comparison of metal abundances in DLAs from optical vs. radio-selected quasars can help to quantify the dust selection effect. Ellison et al. (2001) find slightly more DLAs in the foreground of radio-selected and optically faint quasars than in optically selected and optically bright quasars, in the sense that may be caused by dust obscuration. However, the sample of radio-selected quasars is still small, and neither of these differences is statistically significant. The strongest conclusion that can be drawn at present is that obscuration reduces the number density and/or Ω_{HI} of DLAs at $1.8 < z < 3.5$ in optically selected samples by a factor of two or less. However, the implications of this result for the mean metallicity have not yet been quantified. Abundance studies for a large sample of DLAs in radio-selected and optically faint quasars will help to improve the constraints on the extent of the dust obscuration bias.

3.2. Iron vs. Zinc

All of our analysis has been based on Zn alone, since we believe Zn is a more reliable metallicity indicator for DLAs than Fe, which has been used in some other studies (e.g., Prochaska & Wolfe 1999, 2000; Savaglio 2001; Prochaska et al. 2001a). The main reasons advocated by these studies for using Fe are: (a) the ease of measuring Fe lines compared to the weaker Zn lines; (b) the ability to probe higher redshifts ($z > 3.5$) with Fe than with Zn;

and (c) the better understanding of the nucleosynthetic origin of Fe than of Zn. We address these issues one by one. (a) As our ability to measure weak absorption lines is getting better in the present age of large telescopes, Zn measurements are becoming easier. Furthermore, this is not a concern for studies of the global $N(\text{HI})$ -weighted metallicity as the systems that are too weak to give detections of Zn lines do not contribute much to the global metallicity anyway. As our analysis has shown, there would be almost no difference in the results even if the limits could be improved in future studies (as there is little difference whether the limits are treated as detections or zeros). (b) The redshift range $z > 3.5$ accessible with Fe is of some interest since the rate of metallicity evolution at high redshifts could in fact be different from that at low redshifts. However, the redshift range $z > 3.5$ represents only 13% of the cosmic history. Therefore, even though Fe is useful for tracing the early chemical evolution of galaxies, it does not add much to studies of the last 87% of the age of the universe. (c) While the nucleosynthetic origin of Zn is harder to understand than that of Fe, observationally Zn and Fe track each other perfectly well for most Galactic disk and halo stars with metallicities between 10^{-2} solar and solar, the metallicity range relevant to DLAs (e.g., Sneden, Gratton, & Crocker 1991). Some models of massive star explosive nucleosynthesis, such as the neutrino-driven wind models (e.g., Hoffman, Woosley, & Qian 1997) provide ways to understand the origin of Zn and the reason for the tight correlation between Fe and Zn in Galactic stars. Thus, there is no strong reason to suspect that the use of Zn biases studies of cosmic chemical evolution in any significant way.

On the other hand, the well-known problem with Fe is its strong depletion on dust grains. Moreover, as with many other elements, the depletion of Fe differs substantially between the cool and warm diffuse interstellar gas, but is strong in both phases (see, e.g., Savage & Sembach 1996). By comparison, Zn is essentially undepleted in the warm interstellar clouds and depleted ~ 40 times less than Fe in the cool interstellar clouds. It is difficult to model unambiguously the dust depletion effects for Fe, because the structure and composition of the dust grains present in the DLAs is not known a priori. Furthermore, the line of sight can pass through a mixture of warm and cold gas, so that the dust depletion within a given DLA can be quite different in different parts of the absorbing gas. Even after averaging over a number of DLAs at a given redshift, it is possible that the mean correction for dust depletion may itself change as a function of redshift. Indeed, as the interstellar metallicity of the DLA galaxies rises with decreasing redshift, their dust-to-gas ratio should also rise more or less in step with the metallicity. Such a redshift-dependent dust depletion can introduce an error in estimates of the metallicity-redshift relation based on Fe data alone, or on a combination of Fe and Zn data. Although the extent of this error is hard to quantify and, in fact, may turn out to be small, it is safer to focus on an element such as Zn that does not have this problem in the first place.

3.3. Future Work

Part of the reason our analysis finds a stronger evidence for evolution than previous studies such as Pettini et al. (1999) is the addition of new data at low redshifts that have recently become available. These new data have resulted in a higher mean metallicity in the lowest redshift bin than found in the earlier analyses. This highlights the need for caution in drawing conclusions from the limited DLA data sets. Indeed, it is obvious that the current samples need significant improvement in the number of measurements at $z < 2$. A large fraction of the Zn measurements so far have focussed on the redshift range $z > 2$. Possible drops in the mean Zn metallicity at $3 < z < 3.5$ and the mean Fe metallicity at $3.5 < z < 4.5$ have been suggested (although on the basis of small samples) by Pettini et al. (1997) and Prochaska & Wolfe (2002), respectively. If verified with future data, a drop in the mean metallicity at high redshifts could signal the epoch of the onset of star formation in DLAs. It is, nevertheless, also essential to increase substantially the lower redshift samples, since the redshift range $z < 2$ probes the cosmic epochs when the bulk of the metals in galaxies were produced. At present, Zn measurements exist for only seven absorbers at $z < 1$ and only two absorbers at $z < 0.5$. This is especially problematic because the redshift ranges $z < 1$ and $z < 0.5$ represent 57% and 37%, respectively, of the age of the universe. Even the number of measurements at $1 < z < 2$ is somewhat limited. Clearly, it is crucial to increase the number of Zn measurements at low and intermediate redshifts. This requires more measurements at $z < 0.6$ with the *Hubble Space Telescope* (HST) and at $0.6 < z < 2$ with ground-based telescopes. It is particularly important to study the high- $N(\text{HI})$ systems since, as we have emphasized here, these systems dominate the global metallicity.

The large numbers of quasar spectra becoming available with surveys such as the Sloan Digital Sky Survey and the FIRST survey will increase the sample of known DLAs and 21-cm absorbers by a large factor. Obtaining element abundances of these new DLAs will be of great importance for pinning down the metallicity-redshift relation for DLAs. Zn abundances in DLAs in front of quasars of different apparent magnitudes and colors will provide constraints on the amount of dust obscuration. Accurate determination of the metallicity-redshift relation for DLAs will, thus, be important for quantifying the selection effects in samples of quasar absorbers and for understanding the nature of DLAs, in addition to providing important constraints on the global star formation history of galaxies.

We thank Eric Feigelson for providing the astronomical survival analysis package ASURV and for helpful discussions. We thank Hsiao Wen Chen, Edward Jenkins, Max Pettini, Jason X. Prochaska, and an anonymous referee for helpful comments. VPK acknowledges partial support from a Research and Productive Scholarship award from the University of South Car-

olina, from the University of South Carolina Research Foundation, and from NASA/South Carolina Space Grant Consortium. SMF thanks the Carnegie Observatories for hospitality during the later phases of this project.

A. APPENDIX

Here, we estimate the global mean interstellar metallicity of galaxies at the present epoch from emission-line observations of H II regions. As an approximation to the mass-weighted mean metallicity, required for models of cosmic chemical evolution, we compute the luminosity-weighted mean metallicity, since the latter is much simpler to evaluate than the former. The luminosity-weighted mean interstellar metallicity of galaxies can be expressed in the form

$$\bar{Z} = \frac{\int Z(L) L \phi(L) dL}{\int L \phi(L) dL}, \quad (\text{A1})$$

where $Z(L)$ is the average interstellar metallicity in a galaxy of luminosity L , and $\phi(L)$ is the luminosity function of galaxies of all morphological types. To evaluate equation (A1), we adopt a Schechter function for $\phi(L)$ and a power law for $Z(L)$, i.e.,

$$\phi(L)dL = \phi^*(L/L^*)^\alpha \exp(-L/L^*)dL/L^*, \quad (\text{A2})$$

and

$$Z(L) = (L/L^*)^\beta Z^*, \quad (\text{A3})$$

where Z^* is the mean metallicity of galaxies with luminosity L^* . Thus, we obtain

$$\bar{Z} = \frac{\Gamma(\alpha + \beta + 2)}{\Gamma(\alpha + 2)} Z^*. \quad (\text{A4})$$

For the parameters of the luminosity function, we adopt the results of Loveday et al. (1992), i.e., $\phi^* = 5.9 \times 10^{-3} h_{75}^3 \text{ Mpc}^{-3}$, $\alpha = -0.97$, and $L^* = 2.3 \times 10^{10} h_{75}^{-2} L_\odot$ (corresponding to $M_B^* = -20.42$ for $H_0 = 75 h_{75} \text{ km s}^{-1} \text{ Mpc}^{-1}$). For the relation between mean metallicity and luminosity, we adopt the parameters $Z^* = 0.90 Z_\odot$ and $\beta = 0.42$, which provide an adequate fit to the data for [O/H] from H II regions vs. M_B in a sample of 39 nearby spiral galaxies from Zaritsky, Kennicutt, & Huchra (1994) and 20 irregular galaxies from Skillman, Kennicutt, & Hodge (1989) and references therein. Inserting these parameters in equation (A4), we obtain the mean interstellar metallicity of nearby galaxies $\bar{Z} \approx 0.8 Z_\odot$.

REFERENCES

- Anders, E., & Grevesse, N. 1989, *Geochim. Cosmochim. Acta*, 53, 197
- Bechtold, J., Siemiginowska, A., Aldcroft, T. L., Elvis, M., & Dobrzycki, A. 2001, *ApJ*, 562, 133
- Bevington, P. R. & Robinson, D. K. 1992, *Data Reduction and Error Analysis for the Physical Sciences*, (New York: McGraw-Hill)
- Boissé, P., Le Brun, V., Bergeron, J. & Deharveng, J.-M. 1998, *A&A*, 333, 841
- de la Varga, A., Reimers, D., Tytler, D., Barlow, T., & Burles, S. 2000, *A&A*, 363, 69
- Edmunds, M. G., & Phillipps, S. 1997, *MNRAS*, 292, 733
- Ellison, S. L. & Lopez, S. 2001, *A&A*, 380, 117
- Ellison, S. L. Yan, L., Hook, I. M., Pettini, M., Wall, J. V., & Shaver, P. 2001, *A&A*, 379, 393
- Fall, S. M., Pei, Y. C., & McMahon, R. G. 1989, *ApJ*, 341, L5
- Fall, S. M., & Pei, Y. C. 1993, *ApJ*, 402, 479
- Fall, S. M. 2001, in *The Extragalactic Infrared Background and its Cosmological Implications*, IAU Symposium, 204, ed. M. Harwit and M. G. Hauser, (ASP: San Francisco), 40
- Feigelson, E. D. & Nelson, P. I. 1985, *ApJ*, 293, 192
- Ge, J., Bechtold, J., & Kulkarni, V. P. 2001, *ApJ*, 547, L1
- Hoffman, R. D., Woosley, S. E., & Qian, Y.-Z. 1997, *ApJ*, 482, 951
- Isobe, T. & Feigelson, E. D. 1990, *BAAS*, 22, 917
- Junkkarinen, V. T., Cohen, R. D., Beaver, E. A., Burbidge, E. M., Lyons, R. W., & Madejski, G. 2002, *ApJ*, submitted
- Kulkarni, V. P., Huang, K., Green, R. F., Bechtold, J., Welty, D. E., & York, D. G. 1996, *MNRAS*, 279, 197
- Kulkarni, V. P., Fall, S. M. & Truran, J. W. 1997, *ApJ*, 484, L7

- Kulkarni, V. P., Bechtold, J., & Ge, J. 1999, in Proc. of ESO Conference on Chemical Evolution from Zero to High Redshifts, ed. J. R. Walsh and M. R. Rosa, (Berlin: Springer-Verlag), 275
- Lanzetta, K. M., Wolfe, A. M., & Turnshek, D. A. 1995, *ApJ*, 440, 435
- Levshakov, S. A., Agafonova, I. I., Centurin, M., & Mazets, I. E. 2002, *A&A*, 383, 813
- Lilly, S. J., Le Fevre, O., Hammer, F., & Crampton, D. 1996, *ApJ*, 460, L1
- Lopez, S., Reimers, D., Rauch, M., Sargent, W. L. W. & Smette, A. 1999, *ApJ*, 513, 598
- Lopez, S., Reimers, D., D’Odorico, S., & Prochaska, J. X. 2002, *A&A*, 385, 778
- Loveday, J., Peterson, B. A., Efstathiou, G., & Maddox, S. J. 1992, *ApJ*, 390, 338
- Lu, L., Savage, B. D., Tripp, T. M., & Meyer, D. M. 1995, *ApJ*, 447, 597
- Lu, L., Sargent, W. L. W., Barlow, T. A., Churchill, C. W., & Vogt, S. S. 1996, *ApJS*, 107, 475
- Madau, P., Ferguson, H. C., Dickinson, M. E., Giavalisco, M., Steidel, C. C., & Fruchter, A. 1996, *MNRAS*, 283, 1388
- Madau, P., Pozzetti, L., & Dickinson, M. 1998, *ApJ*, 498, 106
- Malaney, R. A., & Chaboyer, B. 1996, *ApJ*, 462, 57
- Meyer, D. M., & York, D. G. 1992, *ApJ*, 399, L121
- Meyer, D. M., Lanzetta, K. M., & Wolfe, A. M. 1995, *ApJ*, 451, L13
- Molaro, P., Bonifacio, P., Centurion, M., D’Odorico, S., Vladilo, G., Santin, P., & Di Marcantonio, P. 2001, *ApJ*, 541, 5
- Pei, Y. C., Fall, S. M., & Bechtold, J. 1991, *ApJ*, 378, 6
- Pei, Y. C. 1992, *ApJ*, 395, 130
- Pei, Y. C. & Fall, S. M. 1995, *ApJ*, 454, 69
- Pei, Y. C., Fall, S. M., & Hauser, M. G. 1999, *ApJ*, 522, 604
- Petitjean, P., Srianand, R., & Ledoux, C. 2000, *A&A*, 364, L26
- Pettini, M., Smith, L. J., Hunstead, R. W., & King, D. L. 1994, *ApJ*, 426, 79

- Pettini, M., Smith, L. J., King, D. L., & Hunstead, R. W. 1997, *ApJ*, 486, 665
- Pettini M., Ellison, S. L., Steidel, C. C., & Bowen, D. V. 1999, *ApJ*, 510, 576
- Pettini, M., Ellison, S. L., Steidel, C. C., Shapley, A. E., Bowen, D. V. 2000, *ApJ*, 532, 65
- Prochaska, J. X., & Wolfe, A. M. 1996, *ApJ*, 470, 403
- Prochaska, J. X., & Wolfe, A. M. 1997, *ApJ*, 474, 140
- Prochaska, J. X., & Wolfe, A. M. 1999, *ApJS*, 121, 369
- Prochaska, J. X., & Wolfe, A. M. 2000, *ApJ*, 533, L5
- Prochaska, J. X., Gawiser, E., & Wolfe, A. M. 2001a, *ApJ*, 552, 99
- Prochaska, J. X. et al. 2001b, *ApJS*, 137, 21
- Prochaska, J. X., & Wolfe, A. M. 2002, *ApJ*, 566, 68
- Savage, B. D. & Sembach, K. R. 1996, *ARAA*, 34, 279
- Savaglio, S. 2001, in *The Extragalactic Infrared Background and its Cosmological Implications*, IAU Symposium, 204, ed. M. Harwit and M. G. Hauser, (ASP: San Francisco), 24
- Skillman, E. D., Kennicutt, R. C., & Hodge, P. W. 1989, *ApJ*, 347, 875
- Snedden, C., Gratton, R. G., & Crocker, D. A. 1991, *A&A*, 246, 354
- Somerville, R. S., Primack, J. R., & Faber, S. M. 2001, *MNRAS*, 320, 504
- Tissera, P. B., Lambas, D. G., Mosconi, M. B., & Cora, S. 2001, *ApJ*, 557, 527
- Vladilo, G., Bonifacio, P., Centurion, M., & Molaro, P. 2000, *ApJ*, 543, 24
- Wolfe, A. M., Lanzetta, K. M., Foltz, C. B., & Chaffee, F. H. 1995, *ApJ*, 454, 698
- Zaritsky, D., Kennicutt, R. C., & Huchra, J. P. 1994, *ApJ*, 420, 87

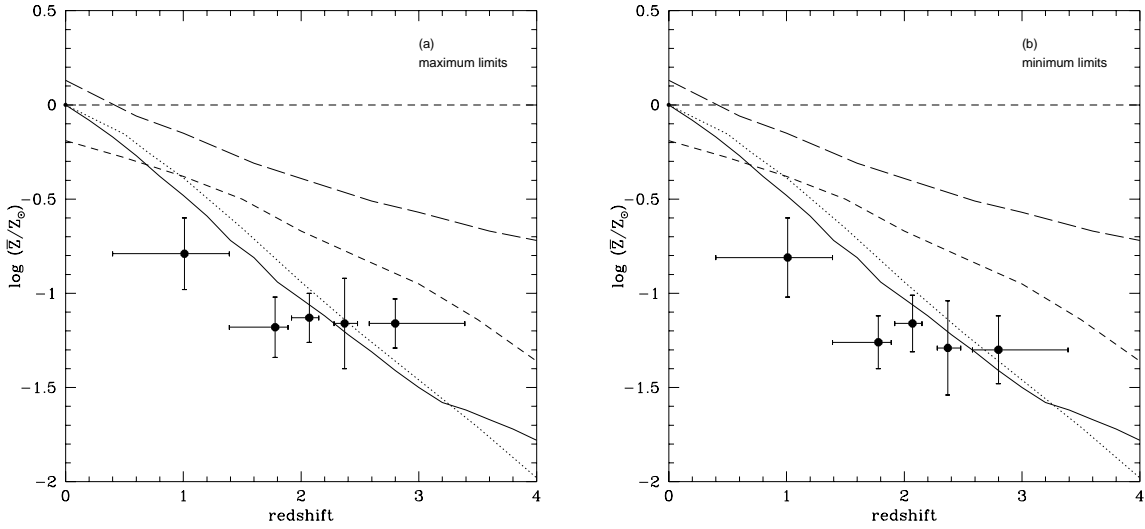


Fig. 1.— The global metallicity-redshift relation deduced from damped Ly- α absorbers. Filled circles show the logarithmic $N(\text{HI})$ -weighted mean Zn metallicity relative to the solar value vs. redshift for measurements from the literature. Left panel (a) includes detections and upper limits treated as detections, while right panel (b) includes detections and upper limits treated as zeros. Vertical error bars denote 1σ uncertainties in the logarithmic $N(\text{HI})$ -weighted mean metallicity. Data points are plotted at the median redshift in each bin. Horizontal bars denote the full range of redshifts of the DLAs in each bin. Horizontal dashed line at $\bar{Z} = Z_{\odot}$ denotes the solar level. Dotted, short-dashed, solid, and long-dashed curves show, respectively, the ‘true’ mean metallicity (not corrected for dust obscuration) expected in the cosmic chemical evolution models of Pei & Fall (1995), Malaney & Chaboyer (1996), Pei et al. (1999), and Somerville et al. (2001). See text for further details.

TABLE 1
Previous Studies of Global Metallicity Evolution in DLAs

Ref. [†]	Element	Detections, Limits, Treatment ^{††}	z range	Data binned?	Errors in weighted \bar{Z} ?	Slope fitted?	Evolution?
1	Zn	19, 15, D	0.7 – 3.4	Yes	No	No	No
2	Zn	24, 16, D	0.4 – 3.4	Yes	No	No	No
3	Zn	11, 4, D	1.8 – 2.6	Yes	No	No	No
3	Fe	19, 1, D	1.8 – 4.2	Yes	No	No	No
4	Zn	28, 0, E	0.4 – 3.4	Yes	No	–0.13 ± 0.07	No
5	Fe	39, 0, E	1.8 – 4.2	Yes	Yes	No	No
6	Zn, Fe*	75, 0, E	0 – 4.4	Yes	No	No	No
7	Fe*	35, 0, E	1.8 – 4.5	Yes	Yes	No	No
8	Fe	51, 0, E	1.6 – 4.5	Yes	Yes	No	No
8	Zn	10, 5, D	1.6 – 2.8	Yes	Yes	No	Possible**
This work	Zn	36, 21, D,Z,S	0.4 – 3.4	Yes, No	Yes	–0.26*** ± 0.10	Likely

[†] References: 1. Pettini et al. (1997); 2. Pettini et al. (1999); 3. Prochaska & Wolfe (1999); 4. Vladilo et al. (2000); 5. Prochaska & Wolfe (2000); 6. Savaglio (2001); 7. Prochaska, Gawiser, & Wolfe (2001a); 8. Prochaska & Wolfe (2002).

^{††} D: Limits treated as detections; E: Limits Excluded; Z: Limits treated as zeros; S: Limits treated with survival analysis.

*: Sometimes other elements (Cr, Ni, Si etc.) used as a proxy for Fe or Zn.

**: But Prochaska & Wolfe (2002) state that this may be because of the small sample size.

***: Value obtained with survival analysis.

TABLE 2
Global Zn Metallicity vs. Redshift (Binned)

z range	Detections, Limits	Median z	$\log(\bar{Z}/Z_{\odot})$ Max. Limits	$\log(\bar{Z}/Z_{\odot})$ Min. Limits	$\log(\bar{Z}/Z_{\odot})$ Survival Analysis
0.40-1.39	9, 2	1.01	-0.79 ± 0.19	-0.81 ± 0.21	-0.80 ± 0.12
1.39-1.89	7, 4	1.78	-1.18 ± 0.16	-1.26 ± 0.14	-1.23 ± 0.10
1.92-2.15	8, 4	2.07	-1.13 ± 0.13	-1.16 ± 0.15	-1.16 ± 0.15
2.28-2.48	8, 3	2.38	-1.16 ± 0.24	-1.29 ± 0.25	-1.22 ± 0.09
2.58-3.39	6, 6	2.80	-1.16 ± 0.13	-1.30 ± 0.18	-1.25 ± 0.20

TABLE 3
Exponential Fits to Global Metallicity-Redshift Relation

Binning	Treatment of Limits	$\log(\bar{Z}_0/Z_\odot)$	b
Unbinned	Maximum limits	-0.71 ± 0.20	-0.20 ± 0.11
Unbinned	Minimum limits	-0.64 ± 0.20	-0.27 ± 0.12
Binned	Maximum limits	-0.76 ± 0.27	-0.16 ± 0.12
Binned	Minimum limits	-0.72 ± 0.30	-0.23 ± 0.15
Binned	K-M Survival Analysis	-0.64 ± 0.20	-0.26 ± 0.10

TABLE 4
Fits of Chemical Evolution Models to Metallicity-Redshift Relation

Model	Limits	χ^2_ν
Pei & Fall (1995)	Maximum Limits	2.69
	Minimum Limits	3.07
Malaney & Chaboyer (1996)	Maximum Limits	3.67
	Minimum Limits	4.47
Pei et al. (1999) Maximum IRB	Maximum Limits	2.13
	Minimum Limits	2.40
Pei et al. (1999) Optimum IRB	Maximum Limits	1.97
	Minimum Limits	2.18
Pei et al. (1999) Minimum IRB	Maximum Limits	1.76
	Minimum Limits	1.87
Somerville et al. (2001)	Maximum Limits	14.54
	Minimum Limits	17.65